

# Mapping rice-planted areas using time-series synthetic aperture radar data for the Asia-RiCE activity

Kei Oyoshi<sup>1</sup> · Nobuhiro Tomiyama<sup>2</sup> · Toshio Okumura<sup>2</sup> · Shinichi Sobue<sup>2</sup> · Jun Sato<sup>3</sup>

Received: 4 August 2015 / Revised: 23 October 2015 / Accepted: 11 November 2015 / Published online: 23 November 2015  
© The International Society of Paddy and Water Environment Engineering and Springer Japan 2015

**Abstract** In Asia, rice is a staple cereal crop and the continent accounts for about 90 % of the global rice production and consumption. Statistics on the areas planted with rice or production of paddy rice are fundamental to agriculture-related decisions or policy-making. Asia-Rice Crop Estimation & Monitoring (Asia-RiCE) aims to develop rice-related information, such as paddy field maps, rice growing conditions, yield, and production, using remote sensing tools and disseminate the same at the local and global scales. In this paper, we propose a methodology for the identification of rice-planted areas by using multi-temporal SAR images; a software named International Asian Harvest mOnitoring system for Rice (INAHOR) was developed to manipulate the proposed algorithm. The INAHOR uses the imagery observed both at the time of planting of rice and grown-up stages. In this study, two thresholds needed for the INAHOR were optimized based on the detailed land cover data collected through a field survey. Rice-planted areas across the study area in Japan were identified by the INAHOR using the RADARSAT-2 Wide Fine beam mode data. The classification results of RADARSAT-2 VV and VH polarizations were compared. The data with VH polarization showed a higher total accuracy of 83 % with  $-20.5$  dB and  $3.0$  dB for the

minimum and range thresholds, respectively. The INAHOR is currently being used with the RADARSAT-2, ALOS, and ALOS-2 SAR data in the Southeast Asian countries to assess the robustness of the thresholds and classification accuracies under the framework of Asia-RiCE.

**Keywords** Asia-RiCE · GEOGLAM · INAHOR · Paddy field · Synthetic aperture radar (SAR)

## Introduction

Rapid population growth, economic growth and a corresponding shift to meat-rich diets, and the increase in extreme weather events reflect on the increasing importance of global food security. In recent years, global food prices have increased and short-term volatility is emerging. This excessive volatility has had a negative impact on world's poorest region in terms of their access to food and livestock producers (G20 Agricultural Minister 2011). In order to ensure global food security, by improving market transparency through dissemination of information, and to reduce the volatility in food prices, Group on Earth Observations (GEO) Global Agricultural Monitoring (GLAM) was endorsed in the final declaration of the 2011, G20 Cannes Summit (G20 Summit 2011). GEOGLAM aims to reinforce the international community's capacity to produce and disseminate reliable, accurate, timely, and sustained crop monitoring information, and yield forecasts at national, regional, and global scales by using coordinated Earth observations from satellites and integrate them with the ground-based and other in situ measurements (GEO 2011; Whitcraft et al. 2015). Crop condition reports, called "Crop Monitor," based on agricultural statistical

✉ Kei Oyoshi  
ohyoshi.kei@jaxa.jp

<sup>1</sup> Earth Observation Research Center, Japan Aerospace Exploration Agency, 2-1-1 Sengen, Tsukuba, Ibaraki 305-8505, Japan

<sup>2</sup> Remote Sensing Technology Center of Japan, 3-17-1 Toranomon, Minato-ku, Tokyo 105-0001, Japan

<sup>3</sup> National Institute of Technology, Tsuruoka College, 104 Sawada, Inooka, Tsuruoka, Yamagata 997-8511, Japan

inputs, satellite-derived status of crop growth, and agro-meteorological information have been provided by GEOGLAM to the Agricultural Market Information System (AMIS) on a monthly basis since September 2013 (AMIS 2013).

GEOGLAM covers four major cereal crops: wheat, maize, soybeans, and rice. Since rice has been a staple food for many Asian countries and 90 % of the global rice are produced and consumed in this continent, agencies associated with the Asian space and agricultural activities launched Asia-Rice Crop Estimation & Monitoring (Asia-RiCE) component for the GEOGLAM initiative in 2011. Asia-RiCE aims to develop and disseminate rice-related information such as the spatial distribution of paddy fields, rice growing conditions, yield, and production (Asia-RiCE 2012). Technology Demonstration Sites (TDS) were established in each participating country to develop and demonstrate the rice monitoring technology using satellite and in situ observation data.

Statistics on the area planted with rice or its production are fundamental to agriculture-related decisions or policy-making. However, it is expensive and time consuming to periodically collect and maintain agricultural data at the provincial or national level. Furthermore, in some regions in Southeast Asia, rice can be planted and harvested more than twice in a year and the crop calendar is quite complicated (Sakamoto et al. 2006). Therefore, earth observation satellites play an important role in estimating rice-planted areas in a timely, efficient, accurate, and objective manner.

Rice is mainly cultivated in the rainy season, and a high density of the cloud cover in this season limits the observations made from the space through optical sensors. However, synthetic aperture radar (SAR) can penetrate the cloud cover and observe the target object even if it is covered with clouds. Hence, usefulness of SAR has been widely demonstrated in terms of the rice monitoring data such as paddy field mapping or retrieval of the biophysical characteristics of rice (Toan et al. 1989; Kurosui et al. 1995; Okamoto and Kawashima 1999; Zhang et al. 2009; Inoue and Sakaiya 2013). However, the interactions between the paddy rice and microwaves strongly depend on the wavelengths (Ka, Ku, X, C, and L) or polarizations (HH, HV, VH, and VV) (Inoue et al. 2002). The algorithm for the identification of the rice-planted areas must, therefore, be optimized and evaluated for selected the wavelength, polarization, and also the date of data acquisition, conditions of the paddy fields including rice varieties, planting density, or field management. In this study, we developed a methodology for the identification of rice-planted areas by using multi-temporal SAR images, and a software named INAHOR was developed to manipulate the developed algorithm. The algorithm uses two thresholds and these were optimized and validated based on the intensive land cover data collected through a field survey. In addition,

the time-series data acquired through the VV and HV polarization modes of RADARSAT-2 were tested and the classification accuracy for each polarization mode was evaluated.

## Methodology

### Algorithm for the identification of rice-planted area

Paddy fields with a transplanting system have unique characteristics, which are different from lands covered with other crops, because paddy fields experience agricultural inundation before transplanting. Figure 1 shows a schematic diagram of the temporal profile of C- or L-band SAR backscatter data over a paddy field.

SAR backscatter from a surface largely depends on the roughness of the surface; this causes a low backscatter during the transplanting stage and a high backscatter during the growing stages. This results in large seasonal changes in the SAR backscatter, and this feature can be utilized for the identification of rice-planted areas. Toan et al. (1997) demonstrated rice crop mapping using ERS-1 SAR data and by assessing the differences in the backscatter of a pair of images; however, they suggested that a quantitative assessment based on the data acquired through extensive field surveys is imperative to confirm the mapping accuracy or propriety of the threshold.

We essentially followed the algorithm proposed by Toan et al. (1997), but assessed the classification accuracies and thresholds based on the land cover data of each parcel in the cropping areas collected through an intensive field survey. We also compared the result from the VV and VH polarizations. Further, a minimum threshold value was employed to reduce mis-classifications of the land covers owing to large changes in the temporal SAR profiles such as deciduous forests or other crops. To identify the rice-planted areas with large variations in their crop calendars, especially in Southeast Asia, the

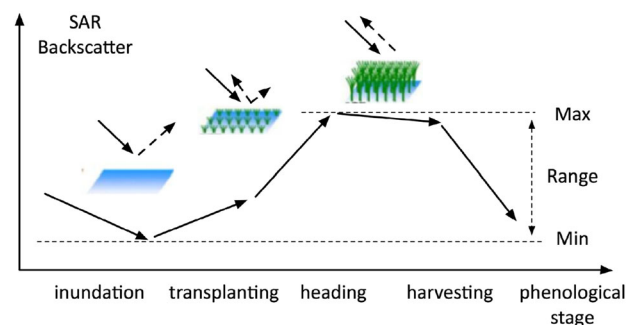


**Fig. 1** Schematic of the seasonal change in SAR backscatter over a paddy field

thresholds of minimum and range values were calculated using several candidate images for both transplanting and grown-up phases captured through an entire rice growing cycle. Therefore, the temporal SAR backscatter profile of a rice-planted pixel is assumed to have a backscattering coefficient less than a certain minimum threshold and greater than a certain range threshold. This algorithm can be expressed as

rice-planted area:  $min < threshold1 \text{ and } range > threshold2$   
 other land covers: *the others*,

where *min* and *range* are the minimum and range values of temporal profiles of backscattering coefficients, respectively. Range value is calculated by subtracting the minimum value from the maximum value.

### International Asian Harvest Monitoring System for Rice

International Asian Harvest monitoring system for Rice (INAHOR) was developed to identify the rice-planted area using the above-mentioned algorithm. INAHOR is run on Linux with simple GUI so that the members in Asia-RiCE or related agencies can easily manipulate the time-series SAR data, and create a rice-planted area map. Rice-planted area and rice production can be estimated if the ancillary boundary or yield data are inputted. Although INAHOR is originally designed for the manipulation of the Advanced Land Observing Satellite-2 (ALOS-2) Phased Array L-band Synthetic Aperture Radar-2 (PALSAR-2), other SAR data with the GeoTIFF and orthorectified data are also applicable.

Figure 2 illustrates the screen captures of INAHOR including the main window (Fig. 2a) and processing procedures. To calculate the minimum and range values in temporal SAR backscatter profiles, a rice cropping cycle must be determined. Firstly, the candidate images for planting and grown-up stages must be selected based on the existing crop calendar (Fig. 2b). Second, the minimum and the range images are created by selecting the minimum values from the candidate planting images and by selecting maximum images from the candidate grown-up images; then the range image is created by subtracting the minimum image from the maximum image. Next, two thresholds for minimum and range values are set (Fig. 2c), and the rice-planted areas are finally identified (Fig. 2d). The resulting rice-planted map can be exported in a GeoTIFF format file. In this processing procedures, minimum and range value thresholds must be evaluated, and this study optimizes these values for the study area based on the land cover data collected by the field survey.

## Study area and data

### Study area

According to the agricultural statistics published by the Ministry of Agriculture, Forestry and Fisheries (MAFF), Japan (2014), the area of rice planting in Japan was 2,280,000 ha in 2013. The areas reached a peak in 1969 with 3,441,000 ha, and it has been decreasing since the 1970s. Yamagata Prefecture located at the northeastern part of Japan is the seventh largest rice-planted prefecture in Japan with 88,300 ha in 2013. Tsuruoka City, located in Yamagata Prefecture, was registered as Japan's TDS site for Asia-RiCE (Fig. 3), and the Shonai Plain, which includes Tsuruoka city, is one of the largest rice-producing areas. For this reason, Tsuruoka City and the surrounding areas were selected as the study site in this study.

Rice cropping system in this area is single cropping and the area is irrigated. The Rice phenological stages of rice in this region are almost homogeneous, most rice plants are transplanted from May to June, and harvested from September to October. Since soybean or other crops are also cultivated in the region, the identification of paddy fields from other crops is imperative for the improvement of the accuracy of the rice-planted area identification.

### RADARSAT-2 data

RADARSAT-2 is a Canadian C-band radar satellite launched in December 2007. RADARSAT-2 has various beam modes, and the Wide Fine beam mode images were used in this study. The data were provided by the Canadian Space Agency (CSA) under the framework of the Science and Operational Applications Research (SOAR) of the Joint Experiment for Crop Assessment and Monitoring (JECAM) program. Eight scenes of RADARSAT-2 Wide Fine beam mode (VV, VH) data were observed and available during April 16, 2014 to July 28, 2014. Specifications of the RADARSAT-2 Wide Fine beam mode are listed in Table 1. The proposed algorithm for the identification of the rice-planted area needs the SAR imagery acquired on both the transplanting and grown-up phases. In this study, the image acquired on May 17, 2014, was selected as the transplanting phase, and those acquired on July 4 and 28 were selected as the grown-up images based on the crop calendar in this region.

### Pre-processing

RADARSAT-2 data were imaged, and corrected radiometrically and geometrically by using the Next ESA SAR

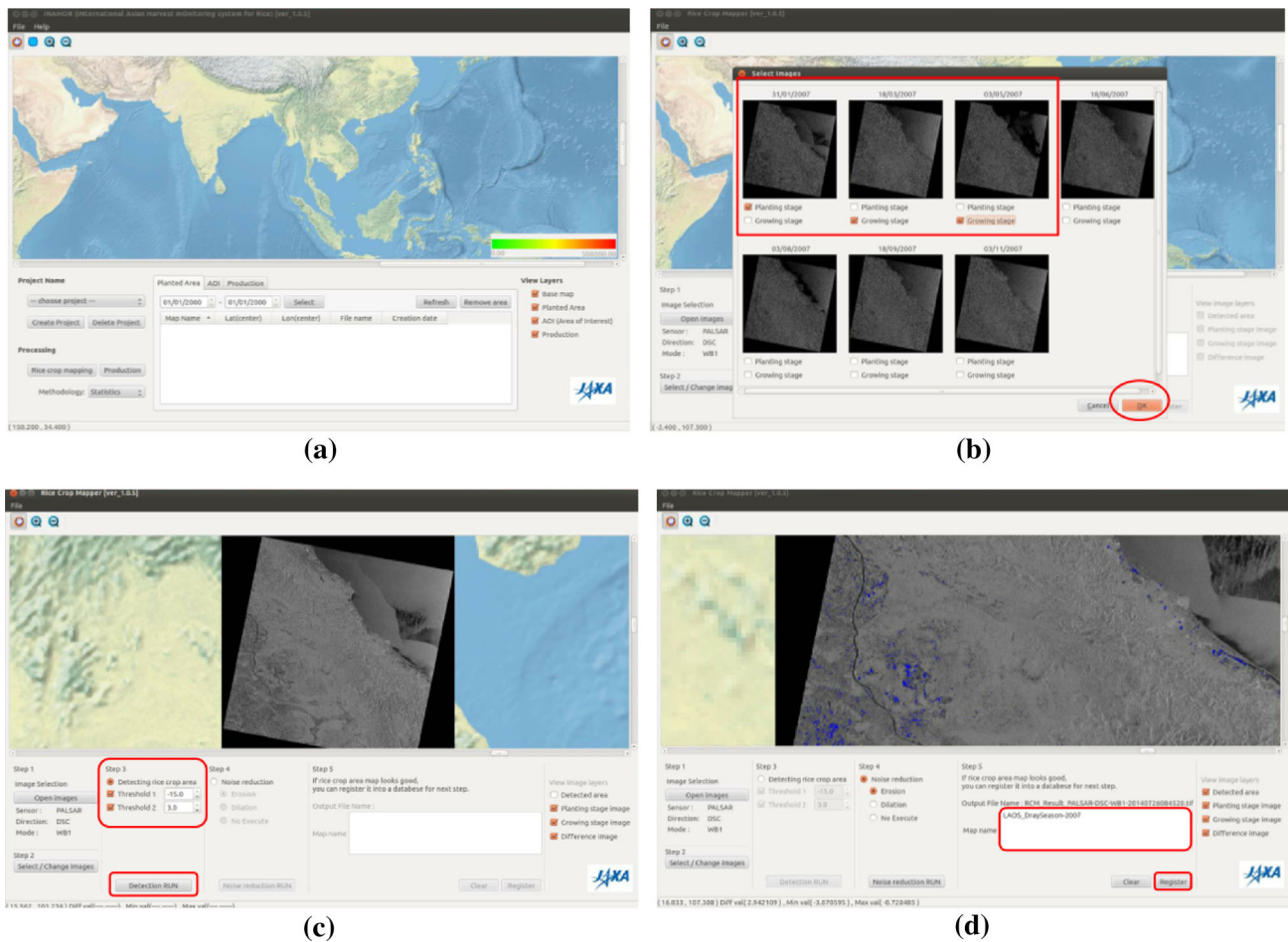
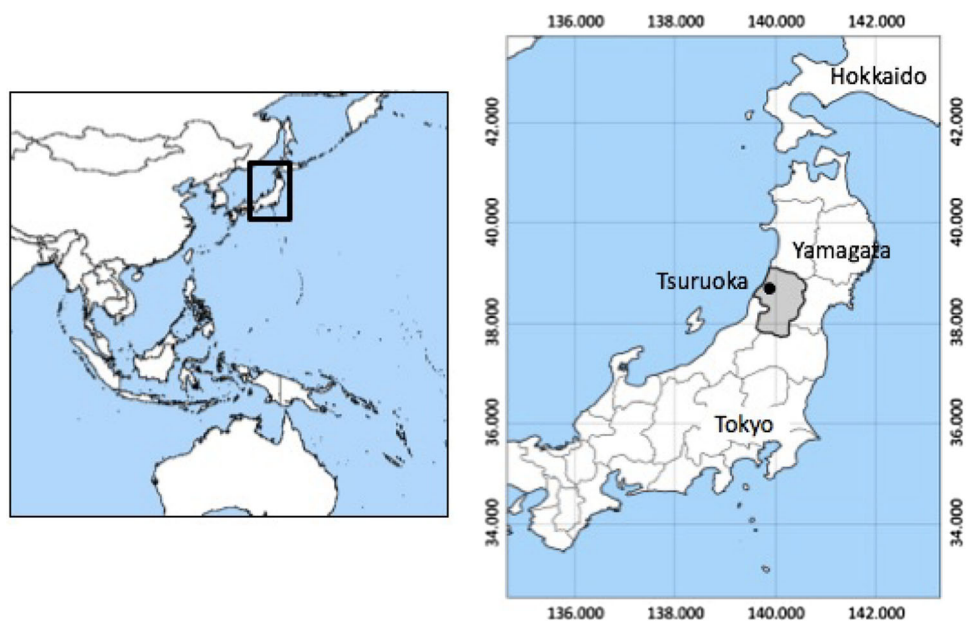


**Fig. 2** Screen captures of the INAHOR software for mapping rice-planted areas. **a** Main window. **b** Selecting images for processing. **c** Setting thresholds. **d** Detected rice-planted areas

**Fig. 3** Location of the study area, Tsuruoka city, Yamagata prefecture, Japan





Toolbox (NEST) with the 50-m digital elevation model data, which is developed by the geospatial information (GSI) Authority of Japan. The digital number data were converted to gamma-naught (dB), and the data were resampled to a spatial resolution of 8.0 m by applying the nearest-neighbor algorithm. Then, the median filter with a  $3 \times 3$  window was applied to reduce the speckle noise inherent in SAR imagery. Finally, the RADARSAT-2 data were clipped over the area extending from 38.5 to 39.0 N and 139.6 to 140.0E to cover the study area. The temporal profiles of the backscattering of VV and VH over the typical land covers (paddy, other crop, water, forest, urban) are shown in Fig. 4. The temporal profile of paddy rice shows large temporal variations in both VV and VH, which is low during transplanting and high in the grown-up stages.

The minimum value image was composited by selecting the lowest value among the candidate images. However, only the data obtained on May 17, 2014, were selected for the minimum value calculation in this study because the cropping calendar was simple and almost same in the study area. Regarding the calculation of the range value image, firstly the highest value image was composited by selecting the highest value among the candidate grown-up images observed on July 4 and 28. Then, the range value image was calculated by subtracting the minimum value image from the maximum value image.

### Field data collection

Field survey for collecting land cover data with handy GPS was conducted on June 3 and 4, 2014. The collected data were used to model and validate the algorithm for the rice-planted area identification. There were complicated mixtures of paddy rice and other crops such as soybeans; the boundary delineation of the paddy field and other crops was intensively conducted by the parcel of crop-lands. Other land covers including urban, forest, and water area are identified mainly from the Google Earth because these are easily identified by the visual interpretation of the images. Land cover data collected by the field survey and image interpretation are illustrated in Fig. 5. The images on Google Earth around the study area were taken in 2012 and 2013 (accessed on 15th October 2015), and it is confirmed that the selected sample areas have no land cover changes.

### Evaluation of the combination of thresholds

To optimize the thresholds and validate the rice-planted area identification algorithm, 12,000 pixels including 6000 pixels of paddy field and 6000 pixels of other four land covers (each 1500 pixels of other crops, forest, urban, and water area) were randomly selected from the field survey data. As much as 12,000 pixels of the sample dataset were divided into two datasets, each dataset consists of 3000

**Table 1** Specifications of RADARSAT-2 (wide fine beam mode)

Center frequency	5.405 GHz (C-band)
Polarization	HH or VV or HV or VH or HH + HV or VV + VH
Band width	100 MHz
Altitude	798 km
Image width	170 km
Incidence angle	20°–40°
Slant-range resolution	4.7 m (single look complex)
Azimuth-range resolution	5.1 m (single look complex)

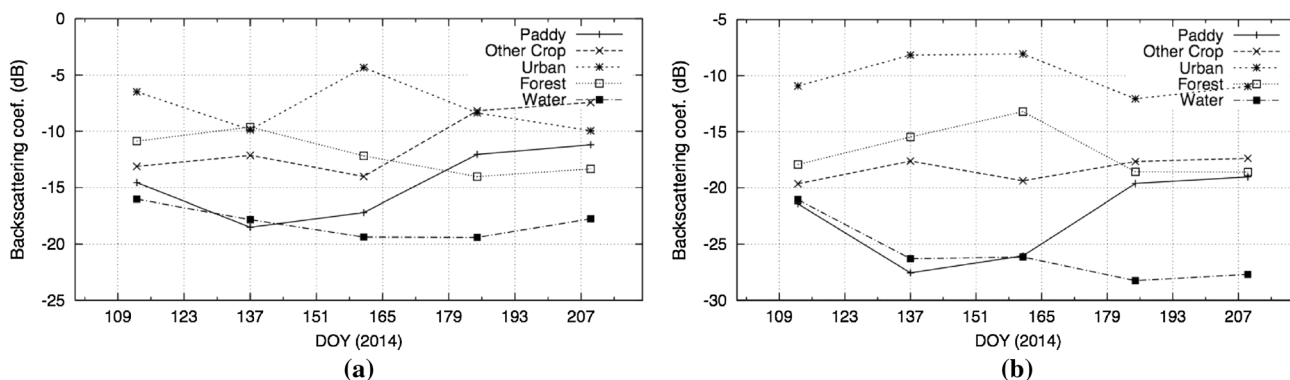


**Fig. 4** Temporal profiles of backscatter coefficient over various land covers. **a** VV polarization, **b** VH polarization

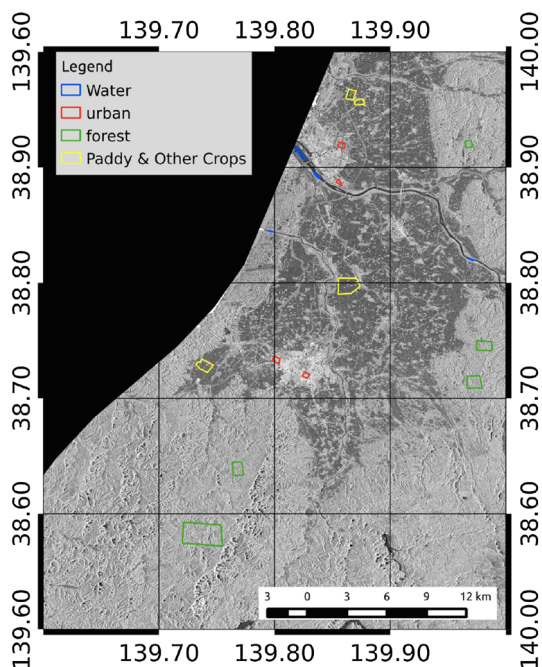


**Fig. 5** Land cover data collected by the field survey and image interpretation

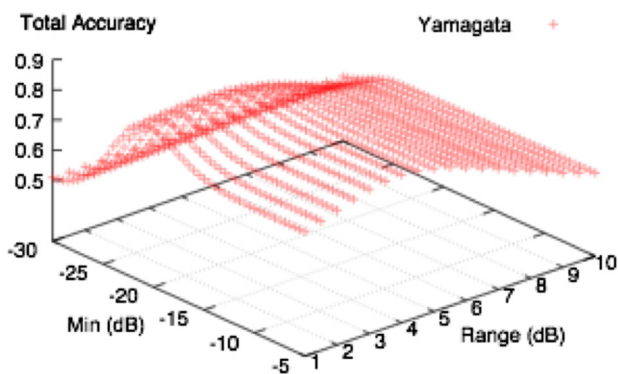


**Fig. 6** Total accuracy as a function of minimum and range thresholds (VH polarization)

pixels of paddy field and 3000 pixels of the four other types of land covers (750 pixels each). One was used as the training dataset for the threshold optimization and the other was used as the test dataset for the validation. A pair of training and test datasets was prepared from both VV and VH polarizations.

Threshold optimization was implemented by testing the combinations of minimum and range values within the certain ranges. Minimum and range value thresholds were tested every 0.5 dB step, and the total accuracies were calculated using the training dataset. Then, the combination of minimum and range values with the highest total accuracy was regarded as the optimized thresholds. Finally, the optimized thresholds were validated using the test dataset. This optimization was applied to both VV and VH data, and the results were compared.

## Results and discussions

### Optimization of thresholds

Figure 6 illustrates the total accuracies of the rice-planted area classification with the training dataset of the VH data as a function of each combination of the minimum and range value thresholds. The highest total accuracy for VH polarization was 83 % with  $-20.5$  dB and 3.0 dB of minimum and range thresholds, respectively. The highest total accuracy for the VV polarization was 76 % with  $-12.5$  dB and 1.0 dB of minimum and range thresholds, respectively. Tables 2 and 3 show the error matrixes of the classification results. VH indicated larger optimization of the range threshold. This implies that VH can capture the large temporal variations of the rice-planted area more clearly.

The histograms of the minimum and range values as for paddy and other land covers in terms of VV and VH backscattering coefficients are shown in Fig. 7. The minimum values of the paddy field are distributed in a

**Table 2** Accuracy assessment of the classification with VH polarization data

	Rice-planted area (pixels)	Other land covers (pixels)	Producer's accuracy
Rice-planted area	2504	496	0.83
Other land covers	517	2483	0.83
User's accuracy	0.83	0.83	0.83

**Table 3** Accuracy assessment of the classification with VV polarization data

	Rice-planted area (pixels)	Other land covers (pixels)	Producer's accuracy
Rice-planted area	2187	813	0.73
Other land covers	613	2387	0.80
User's accuracy	0.78	0.75	0.76

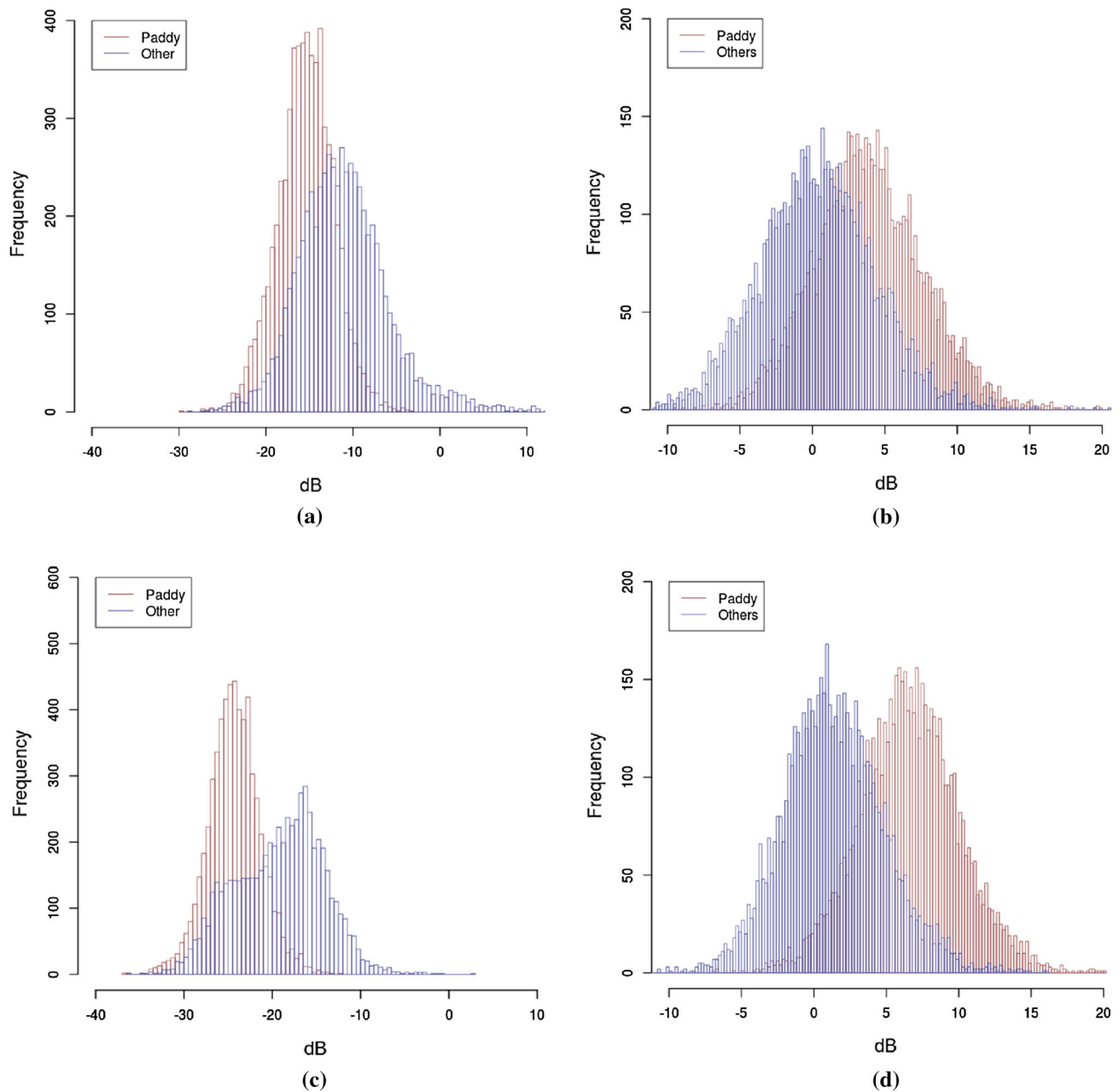


**Fig. 7** Minimum and range value histograms of paddy fields and other land covers as for VV and VH polarizations ( $n = 12,000$ ). **a** Minimum (VV). **b** Range (VV). **c** Minimum (VH). **d** Range (VH)

smaller region, and the range values are distributed in a larger area as compared to other land covers, both in VV and VH polarizations. These results correspond to our assumption of the temporal profile in the SAR backscatter over the paddy field shown in Fig. 1. VH shows higher separability in the minimum and range histograms. Moreover, the C-band VH has higher robustness against the incidence angle variations for the estimation of the rice plant height or biomass (Inoue et al. 2002). It is, therefore, expected that VH can identify the rice-planted area more accurately.

### Rice-planted area mapping

Figure 8 illustrates a map of rice-planted areas generated using VH polarization data from the proposed algorithm with the optimized thresholds. After manipulating the algorithm, a  $3 \times 3$  majority filter with was applied to reduce the remaining speckle noise. Rice-planted areas are widely distributed around the study area in the Shonai plain, but there are areas where other crops are grown or urban areas along the coastal line, which is towards the western part of the study area. Furthermore, there are many

complicated areas where rice and other crops are mixed. One of the mixed areas where we conducted field survey is illustrated in Fig. 9. Although some mis-classified areas remain mainly due to speckle noise, the proposed algorithm could identify rice-planted areas even with a complicated mixture of rice and other crops. The object-based identification algorithm (Peña-Barragán et al. 2011), integrating optical image for the segmentation of each parcel and SAR image for temporal profile, may be useful in reducing mis-classifications induced by speckle noise.

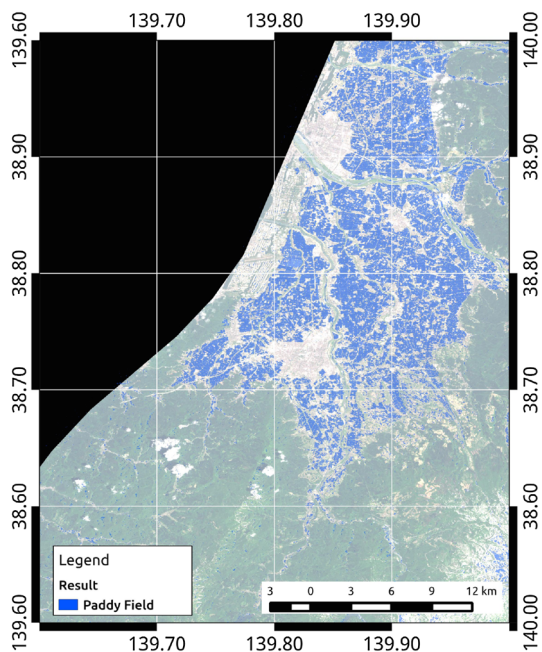


**Fig. 8** Map of rice-planted areas derived from time-series RADAR-SAT-2 VH data over the area around Tsuruoka city, Yamagata prefecture, Japan

## Discussions

Major mis-detected areas were found in sandbars of rivers, and the areas have a temporal backscatter profile similar to that of rice-planted areas. Seasonal changes in river levels cause these temporal backscatter changes over the sandbar. The mis-classification of sandbars as rice-planted areas could be reduced using ancillary water surface mask or land cover data.

This study optimized the thresholds to detect rice-planted areas based on the land cover data collected during the field survey and ancillary satellite data. However, these thresholds may change if the combination of the dates of satellite data acquisition is different and growth stages of the rice are different. Data from highly frequent revisits of less than two weeks may stabilize the thresholds, because the SAR can capture every stage of the rice cropping cycle. Optimized thresholds may also change according to the variety of rice and field management, such as planting density or water level control. Therefore, parameterization and validation of INAHOR in various regions is required to demonstrate the robustness of the software. Moreover, crop calendars are highly complicated in irrigated paddy fields in Southeast Asia, with large temporal and spatial variations (Sakamoto et al. 2006). SAR data used for the INAHOR should be selected by harmonizing the existing crop calendar even if a large amount of SAR data is available. Detailed crop calendars covering two or three times the rice-planted areas with less than 1 km spatial resolution are important to select transplanting and grown-up data appropriately or automatically.

Other wavelengths of SAR data should be demonstrated and compared with this result. In particular, L-band SAR has characteristics similar to that of C-band SAR, but has

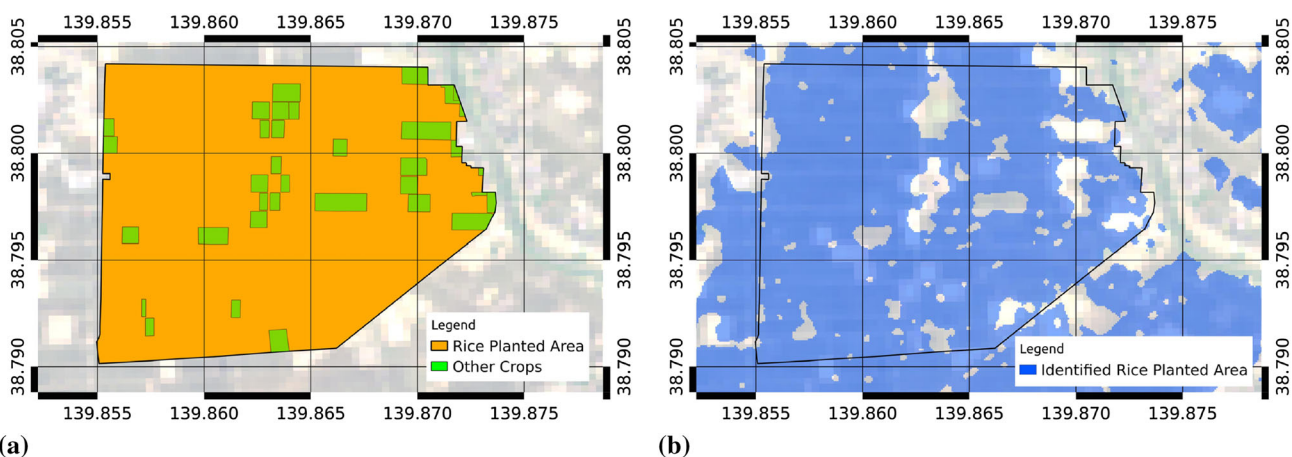


**Fig. 9** Comparison of rice-planted areas identified using SAR data and land cover data collected in a field survey. **a** Example image of field survey area where rice and other crops are co-located. **b** Identified rice-planted area by SAR data with INAHOR



longer wavelength and may be more suitable for detecting water surface under the early vegetative stage of rice. The identification of water surface using SAR data is a key to detect rice-planted areas. Because the INAHOR has been originally designed for L-band SAR, such as ALOS PALSAR and ALOS-2 PALSAR2 (Rosenqvist et al. 2014), it will be tested with L-band SAR data acquired by ALOS-2. The INAHOR is limited in its application to only rice plant with the transplanting system, because the proposed algorithm assumes that rice-planted areas have low backscatter in the transplanting stage. However, several areas in Southeast Asia cultivate rice using the direct seeding system where paddy fields are not filled with water.

Asia-RiCE aims to estimate rice-planted areas or production at provincial to national levels, and the ScanSAR mode (more than 300 km swath) is suitable for covering broad areas. ScanSAR mode observations generally have limited polarization data, only single polarization, and therefore, the INAHOR was designed to utilize single polarization data. However, C- or L-band ScanSAR modes with dual-polarization data are currently being employed: ScanSAR mode of RADARSAT-2, Interferometric Wide Swath (IW) mode of Sentinel-1, and ScanSAR mode of ALOS-2 PALSAR2. These dual-polarization data would be useful not only for mapping rice-planted areas, but also for estimating rice growth stage or biophysical parameters such as plant height and biomass.

## Conclusion

An algorithm for identifying rice-planted areas using time-series SAR data was proposed. This algorithm uses SAR data acquired during the rice planting and grown-up stages to differentiate rice from other crops and land covers. To manipulate the proposed algorithm, the software, INAHOR, was developed. INAHOR employs simple GUI and rice-planted area map can be created by selecting SAR images of rice-transplanting and grown-up seasons and then setting two thresholds for temporal SAR profiles. VV and VH polarizations of RADARSAT-2 wide fine mode data were used to demonstrate the INAHOR over Tsuruoka city in Japan. The two thresholds were optimized on the basis of land cover data collected during a field survey. The classification accuracies were assessed in terms of the combination of the two thresholds and SAR polarizations. As a result, VH showed higher total accuracy of 83 % with  $-20.5$  dB and  $3.0$  dB of minimum and range thresholds, respectively. INAHOR is a potentially powerful tool to deploy Asia-RiCE activities by applying it to other rice-producing countries. In the framework of the Asia-RiCE initiative, INAHOR is currently being demonstrated with RADARSAT-2, ALOS, and ALOS-2 SAR data in Southeast Asian countries and the

robustness of the methodology and classification accuracies is being assessed.

**Acknowledgments** The authors would like to express their gratitude to Mr. Takuma Anahara at the Earth Observation Research Center (EORC), Japan Aerospace Exploration Agency (JAXA) for conducting the field survey, and the Canadian Space Agency (CSA) for providing RADARSAT-2 data through the Science and Operational Applications Research (SOAR)—Joint Experiment of Crop Assessment and Monitoring (JECAM) project.

## References

- Agriculture Market Information System (AMIS) (2013) Market monitor No. 11 September 2013. [http://www.amis-outlook.org/fileadmin/user\\_upload/amis/docs/Market\\_monitor/AMIS\\_Market\\_Monitor\\_Issue\\_11.pdf](http://www.amis-outlook.org/fileadmin/user_upload/amis/docs/Market_monitor/AMIS_Market_Monitor_Issue_11.pdf). Accessed 10 November 2014
- Asia-RiCE (2012) Asia-Rice work plan. <http://www.asia-rice.org/workplan.php>. Accessed 10 November 2014
- G20 Agricultural Ministers (2011) Action plan on food price volatility and agriculture. Meeting of G20 Agricultural Ministers, Paris, France, 22–23 June 2011
- G20 Summit (2011) Cannes Summit final declaration. [https://g20.org/wp-content/uploads/2014/12/Declaration\\_eng\\_Cannes.pdf](https://g20.org/wp-content/uploads/2014/12/Declaration_eng_Cannes.pdf). Accessed 10 Nov 2014
- Group on Earth Observations (GEO) (2011) GEO-GLAM (Global Agriculture Monitoring Initiative). <http://www.earthobservations.org/geoglam.php>. Accessed 10 November 2014
- Inoue Y, Sakaiya E (2013) Relationships between X-band backscattering coefficients from high-resolution satellite SAR and biophysical variables in paddy rice. *Remote Sens Lett* 4(3):288–295
- Inoue Y, Kurosu T, Maeno H, Uratsuka S, Koza T, Dabrowska-Zielinska K, Qi J (2002) Season-long daily measurements of multifrequency (Ka, Ku, X, C, and L) and full-polarization backscatter signatures over paddy rice field and their relationship with biological variables. *Remote Sens Environ* 81:194–204
- Kurosu T, Fujita M, Chiba K (1995) Monitoring of rice crop growth from space using the ERS-1 C-band SAR. *IEEE Trans Geosci Remote Sens* 33(4):1092–1096
- Ministry of Agriculture, Forestry and Fisheries Japan (2014) Crop statistics. [http://www.maff.go.jp/j/tokei/kouhyou/sakumotu/menseki/pdf/menseki\\_sakumotu\\_13.pdf](http://www.maff.go.jp/j/tokei/kouhyou/sakumotu/menseki/pdf/menseki_sakumotu_13.pdf). Accessed 10 November 2014
- Okamoto K, Kawashima H (1999) Estimation of rice-planted area in the tropical zone using a combination of optical and microwave satellite sensor data. *Int J Remote Sens* 20(5):1045–1048
- Peña-Barragán JM, Ngugi MK, Plant RE, Six J (2011) Object-based crop identification using multiple vegetation index, textural features and crop phenology. *Remote Sens Environ* 115:1301–1316
- Rosenqvist A, Shimada M, Suzuki S, Ohgushi F, Tadono T, Watanabe M, Tsuzuku K, Watanabe T, Kamijo S, Aoki E (2014) Operational performance of the ALOS global systematic acquisition strategy and observation plans for ALOS-2 PALSAR-2. *Remote Sens Environ* 155:3–12
- Sakamoto T, Nguyen NV, Ohono H, Ishitsuka N, Yokozawa M (2006) Spatio-temporal distribution of rice phenology and cropping systems in the Mekong Delta with special reference to the seasonal water flow of the Mekong and Bassac rivers. *Remote Sens Environ* 100:1–16
- Toan TL, Laur H, Mougin E, Lopes A (1989) Multitemporal and dual-polarization observations of agricultural vegetation covers by X-Band SAR Images. *IEEE Trans Geosci Remote Sens* 27(6):709–718

- Toan TL, Ribbes F, Wang L, Floury N, Ding K, Kong JA, Fujita M, Takashi K (1997) Rice crop mapping and monitoring using ERS-1 data based on experiment and modeling results. *IEEE Trans Geosci Remote Sens* 35(1):41–56
- Whitcraft AK, Becker-Reshef I, Justice CO (2015) A Framework for Defining Spatially Explicit Earth Observation Requirements for a Global Agricultural Monitoring Initiative (GEOGLAM). *Remote Sens* 7:1461–1481
- Zhang Y, Wang C, Wu J, Qi J, Salas WA (2009) Mapping paddy rice with multitemporal ALOS/PALSAR imagery in southeast China. *Int J Remote Sens* 30(23):6301–6315